An experimental overview of the use of nuclear magnetic resonance imaging to follow solvent ingress into polymers

A. G. Webb* and L. D. Hall

Herchel Smith Laboratory for Medicinal Chemistry, Cambridge University School for Clinical Medicine, University Forvie Site, Robinson Way, Cambridge CB2 2PZ, UK

(Received 23 April 1990; accepted 17 August 1990)

Nuclear magnetic resonance (n.m.r.) imaging has been used to follow the Case I diffusion of benzene, isooctane, acetone and cyclohexane through vulcanized rubber. By using the intrinsic n.m.r. parameters of chemical shift or scalar coupling, separate images can be obtained from two-component solvent mixtures. The use of editing on the basis of n.m.r. relaxation times has been shown not to be applicable in this case. However, methods based on isotopic substitution have been described for systems where chemical shift and scalar coupling behaviour are not able to separate responses.

(Keywords: nuclear magnetic resonance imaging; solvent ingress; Fickian diffusion; chemical shift editing; scalar coupled editing; isotopic substitution)

INTRODUCTION

Polymers can be classified as being in a rubbery or a glassy state, the temperature at which these two states interchange being referred to as the glass transition temperature, T_g. At temperatures above T_g a polymer is found in its rubbery state, i.e. the molecular chains have a large degree of rotational freedom. As the temperature is reduced, the polymer becomes a relatively hard and amorphous glass; there is a sharp change in the physical properties of the polymer, such as tensile strength, elasticity and thermal expansion, and diffusion kinetics in the two states are also very different.

Alfrey *et al.*[1] proposed a classification of the diffusion behaviour of solvents into polymers in three categories:

(1) Case I, or Fickian, diffusion, in which the rate of diffusion of solvents is much less than that of the polymer segmental relaxation rates; this applies to rubbery polymers such as vulcanized rubber (VR). In this case, the distance diffused by a species is proportional to the square root of time.

(2) Case II, or relaxation-controlled, diffusion, in which the rate of diffusion is much greater than that of polymer segmental relaxation; this applies to polymers in the glassy state such as poly(methyl methacrylate) (PMMA). The distance diffused is now directly proportional to time.

(3) Non-Fickian, or anomalous, diffusion, which occurs when the rates of diffusion and segmental relaxation are comparable. In this case the distance diffused is proportional to time raised to a power intermediate between 0.5 and 1.0.

Existing experimental techniques for studying diffusion fall into two main groups: those following the mass uptake of the solvent by the polymer as a function of time, and those measuring the time-dependent concentration profiles of the increased solvent within the polymer. Of the former group, direct weighing methods are by far the most common[2–7]. In the latter group, refractive index measurements are often used for optically transparent polymers[8–10], and a variety of techniques have been used for opaque polymers including the use of composite samples[11], X-ray microradiography[12] and β-particle emission[13]. More recently, n.m.r. imaging has been used by Gummerson *et al.*[14] to study the diffusion of water into permeable rocks and ceramics, and by Rothwell *et al.*[15] to investigate water ingress into polymer composites in order to study the spatial distribution of small cracks that occurred during the manufacturing process. Weisenberger and Koenig[16] and Chu and Foxall[17] have studied the case II diffusion of methanol into PMMA and have found good agreement with the theoretical models proposed. Previous authors[18,19] have also shown that quantitative studies of Case I diffusion can be carried out using n.m.r. imaging.

In the following section we expand upon these studies using the particular exemplar of solvent diffusion into vulcanized rubber (VR). The samples used were sulphur vulcanized at 140°C with *N*-cyclohexyl-2-benzothiazole sulphenamide accelerator present, giving an intermediate crosslinked rubber.

STUDIES OF FICKIAN DIFFUSION USING N.M.R. IMAGING

Since the range of T_g for natural rubber (NR) and its chemical derivatives is approximately -100 to -15°C, all of the n.m.r. experiments carried out at 25°C deal with solvent diffusion that obeys Fick's first law:

$$J = -D\frac{\partial C}{\partial x} \qquad (1)$$

* To whom correspondence should be addressed at Room 45, SAC College of Veterinary Medicine, 1008 West Hazlewood Drive, Urbana, IL 61801, USA

0032-3861/91/162926-13

where J is the flux, i.e. the mass passing through unit area per unit time, D is the diffusion coefficient and x is the distance diffused. This can be converted into a time-dependent differential equation, Fick's second law:

$$\frac{\partial C}{\partial t} = D\frac{\partial^2 C}{\partial x^2} \tag{2}$$

In the ideal case of a semi-infinite sheet, and assuming that D is *independent* of concentration, the solution is given by:

$$C = C_0 \operatorname{erfc} \frac{x}{2(Dt)^{1/2}} \tag{3}$$

where C_0 is the surface concentration and:

$$\operatorname{erfc}(x) = 1 - \frac{2}{\pi^{1/2}} \int_0^x \exp(-\eta^2)\, d\eta \tag{4}$$

In general, however, the diffusion coefficient for polymer–solvent systems displaying Fickian behaviour is concentration-dependent, usually having the form:

$$D = D_0 \exp(kC) \tag{5}$$

where D_0 is the diffusion coefficient corresponding to the surface concentration C_0. We have shown previously[19] that the concentration profiles obtained by ingressing organic solvents into plane sheets of VR are not smooth curves governed by the mathematical function erfc(x) but are sharp, indicating that the diffusion coefficient is concentration-*dependent*. *Figure 1* shows four concentration profiles across a plane sheet of VR through which acetone is diffusing. If the diffusion coefficient is a function of concentration only, a Boltzmann transformation can be applied to equation (2) to give:

$$\left(\frac{\partial x}{\partial t}\right)_C = f(D, C)t^{1/2} \tag{6}$$

Therefore, for a given value of C/C_0, the distance diffused will be proportional to the square root of time, irrespective of the form of the concentration dependence of the diffusion coefficient. The time dependence of the distance diffused can be expressed thus:

$$\text{distance} \propto (\text{time})^n$$

or:

$$\log(\text{distance}) \propto n \log(\text{time})$$

where n theoretically lies between 0.5 for pure Fickian diffusion and 1.0 for pure Case II diffusion. *Figures 2a* and *2b* show plots of log(distance) vs. log(time) for acetone and benzene diffusion, respectively, each for three values of the ratio C/C_0. *Table 1* lists the calculated values for n for all four solvent–polymer systems, showing that the value of n generally lies within experimental error of the theoretical value of 0.5. The calculated values of the diffusion coefficients for the four solvents, using a finite-difference method, are 7.0×10^{-11}, 5.3×10^{-11}, 4.5×10^{-11} and 3.8×10^{-11} m^2 s^{-1} for benzene, cyclohexane, isooctane and acetone, respectively.

The experimental protocol can equally be applied to more technically demanding sample geometries. One such example is the diffusion of decahydronaphthalene (decalin) into ultra-high-molecular-weight polyethylene[20]. A block of the plastic, dimensions $5 \times 5 \times 0.35$ cm, was immersed in decalin at a temperature of 150°C. At a given time the plastic was removed from the solvent and rapidly cooled to 25°C, at which temperature diffusion is negligible. This procedure led to considerable deformation of the sample, but a process of two-dimensional slice selection enables profiles to be obtained across a uniform $0.35 \times 0.35 \times 0.35$ cm^3 cubic volume. A series of concentration profiles are shown in *Figure 3*. It should be stressed that this is a case in which n.m.r. imaging has a distinct advantage over those existing techniques which require a considerable degree of sample homogeneity.

N.m.r. imaging can also be used to study diffusion into

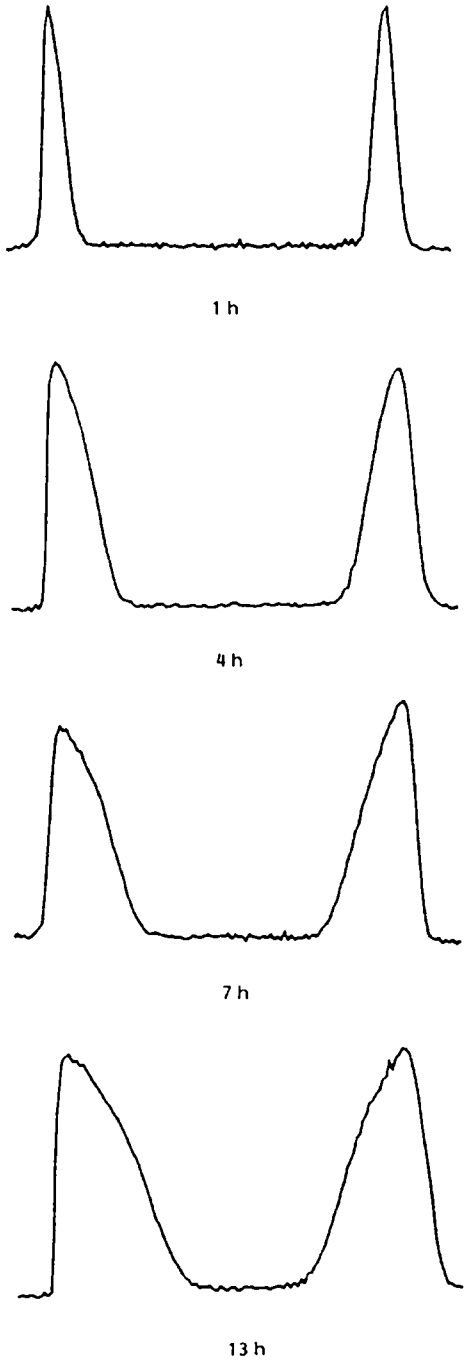

Figure 1 Time course experiment showing the diffusion of acetone into a plane sheet of VR, dimensions $4.3 \times 2.6 \times 1$ cm. Two-dimensional slice selection was used to excite a volume of $0.5 \times 0.5 \times 1.0$ cm^3. Imaging parameters: read-out gradient 4 kHz cm^{-1}, $T_E = 24.8$ ms, $T_R = 1$ s, 256 data points, 32 scans, total experimental time 0.5 min

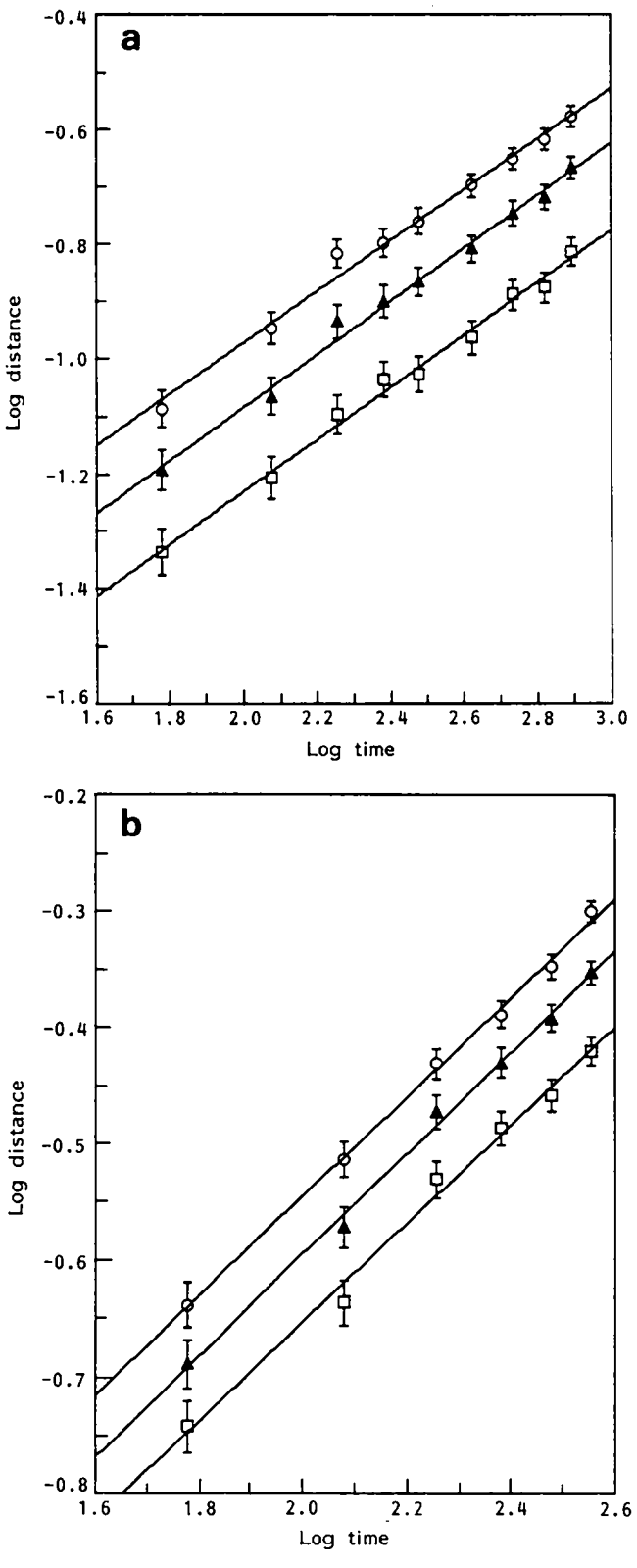

Figure 2 Graphs of log(distance diffused) vs. log(time) for the diffusion of (a) acetone and (b) benzene into a plane sheet of VR for three values of C/C_0: (□) 0.7, (▲) 0.5, (○) 0.3

sample geometries of greater interest with respect to their occurrence in industrial situations. *Figure 4* shows a series of four images following the diffusion of benzene through a cylindrical sample of VR, dimensions $2 \times 2 \times 2.5$ cm. A conventional spin–echo imaging sequence was used, with the offset frequency of the selective 180° refocusing pulse adjusted so as to define a plane through the centre of the cylinder, such that only radial diffusion is detected. *Figure 5* compares the penetration rates of four organic solvents that have been commonly used in studies of diffusion into natural rubber (NR) and its chemical derivatives.

MULTICOMPONENT SOLVENT DIFFUSION

From both an industrial and research point of view an area of considerable interest is the study of multi-component solvent ingress. N.m.r. imaging, in contrast with existing techniques for diffusion measurements, can be simply adapted to separate the responses of different solvents by means of differences in their intrinsic n.m.r. properties. *Table 2* tabulates those n.m.r. properties which are most applicable to editing techniques.

CHEMICAL SHIFT EDITING

If the chemical shift dispersion between peaks is large, and the B_0 homogeneity over the sample is sufficient for each separate peak to be resolved, then chemical shift excitation or suppression techniques can be used to edit the responses from individual components of mixed solvent systems. We have previously shown[21] that a mixed acetone/benzene solvent system can be studied by using a binomial excitation pulse[22] for chemical shift

Table 1 Value of n calculated from n.m.r. data

C/C_0	Acetone	Benzene	Isooctane	Cyclohexane
0.7	0.46±0.06	0.45±0.05	0.52±0.05	0.46±0.06
0.5	0.46±0.05	0.45±0.04	0.49±0.05	0.45±0.07
0.3	0.44±0.04	0.45±0.04	0.45±0.04	0.44±0.06

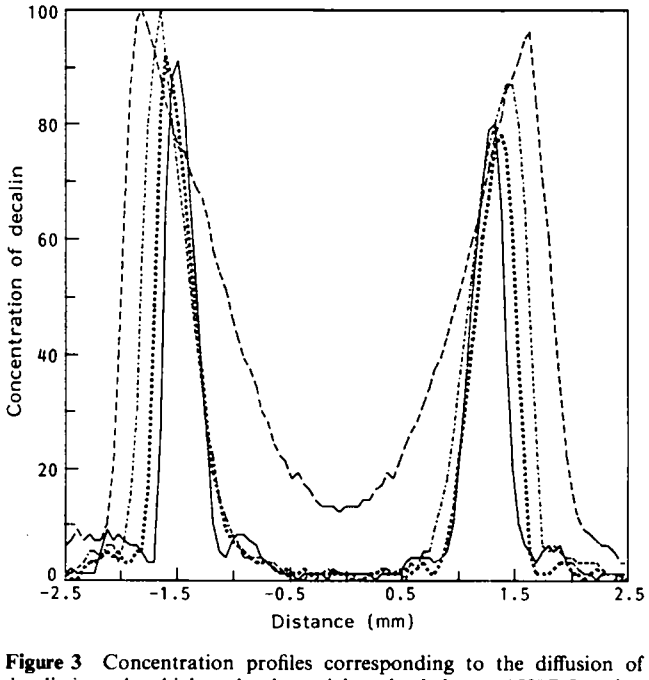

Figure 3 Concentration profiles corresponding to the diffusion of decalin into ultra-high-molecular-weight polyethylene at 150°C. Imaging parameters: read-out gradient 16 kHz cm^{-1}, $T_E = 14.2$ ms, $T_R = 2$ s, 256 data points, 64 scans, total experimental time 2 min. ——, $t = 4.4$ min; · · · · ·, $t = 10$ min; — · — · —, $t = 15$ min; – – – –, $t = 34$ min

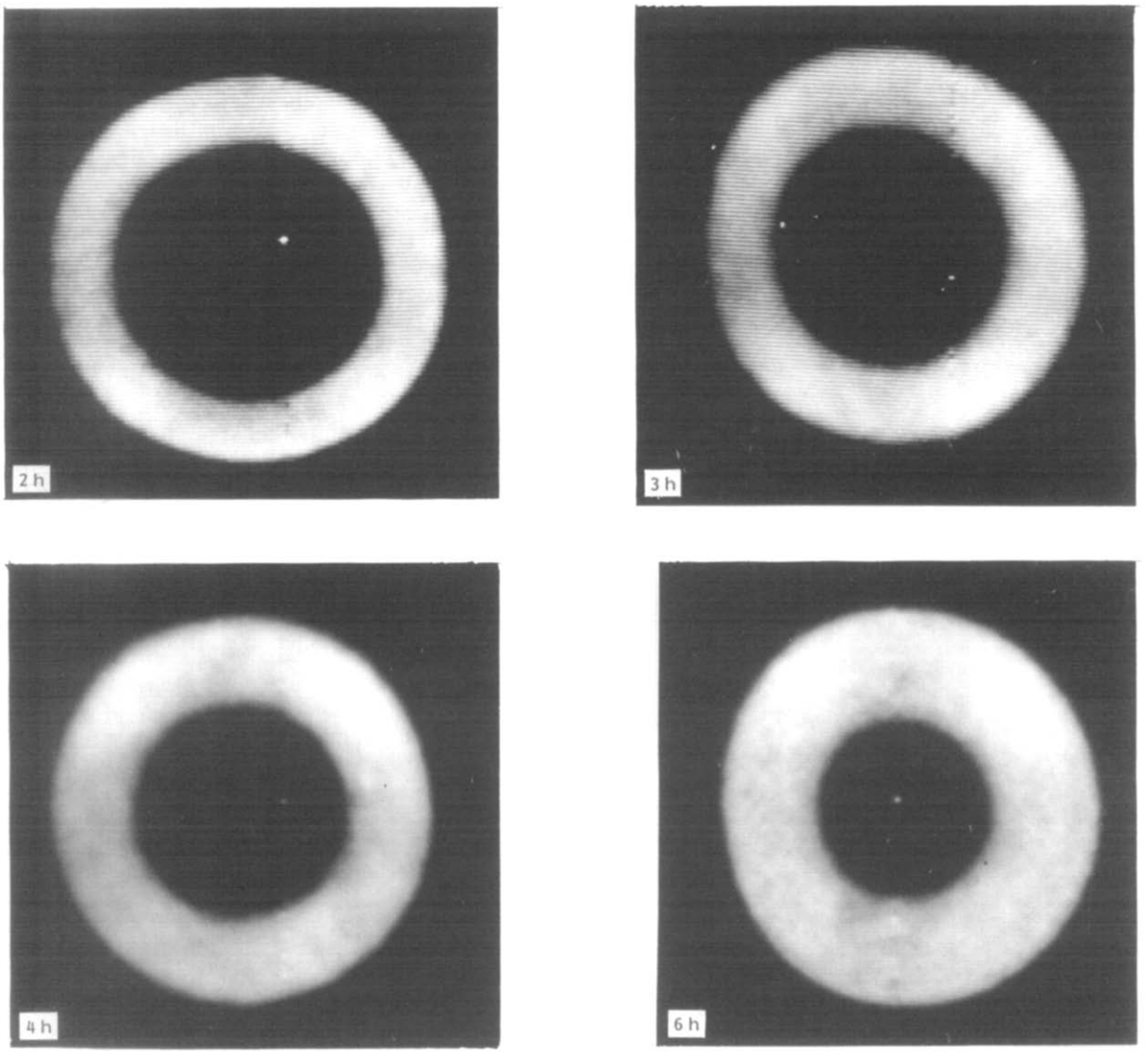

Figure 4 Diffusion of benzene through a cylinder of VR, diameter 2 cm, as a function of time. Imaging parameters: read-out gradient 4 kHz cm $^{-1}$, 128 incremental phase encode steps, slice thickness 0.4 cm, $T_E = 14.2$ ms, $T_R = 2$ s, one scan, total experimental time 2 min

selectivity. *Figure 6* shows the spectroscopic response after application of a binomial excitation pulse to each resonance in turn, using a sample of VR completely saturated with a 1:1 by volume solvent mixture; the response from the suppressed species is less than 5% in each case. This agrees with numerical integration of the product of the frequency response of the binomial pulse sequence and the Lorentzian lineshape of the separate responses with an approximate linewidth of 40 Hz at half height. *Figure 7* shows images from a cylindrical sample of VR, dimensions $1.6 \times 1.6 \times 2.5$ cm, which had been immersed in a 1:1 by volume mixture of benzene and acetone for 4 h. In order to verify the efficacy of replacing the initial 90° excitation pulse with a binomial pulse, one external vial of each of the pure solvents was included in the phantom. *Figure 7A* shows clearly the chemical shift artifact obtained using a conventional spin echo sequence. *Figure 7B* shows the image corresponding to the diffusion of acetone through the sample, and *Figure 7C* that of benzene. The efficacy of suppression is clear from the lack of signal intensity arising from the external vials of pure solvent. It can be seen that the positions of the solvent fronts are identical, the difference in chemical shifts resulting in the slightly different spatial coordinates of the two images.

Figure 8 shows the results of an *ex situ* time course experiment in which the diffusion of a 1:1 by volume mixture of benzene and acetone into VR was followed. Before each measurement, the sample was removed from the solvent mixture, dried and wrapped in plastic film to reduce evaporation. The profiles show that the penetration rates of the two solvents are identical. *Figure 9* shows how this rate compares with that of the single-component solvents, being approximately 2.5 times that of pure acetone and 0.8 times that of pure benzene. These changes can be attributed to the changes in chemical potential of the solvent mixture with respect to the single-component solvents. Similar results are produced from an *in situ* time course experiment and are shown in *Figure 10*; the respective diameters of the glass container and VR cylinder are 4.2 cm and 1.6 cm. It should be noted that the images appear flattened due to screen distortions in the multi-image display mode. Measurements were made on each undistorted image in the single-image display mode.

A second mixed solvent system that was studied was

acetone and water; as in the previous case these two liquids are completely miscible and have only one discrete n.m.r. resonance apiece. The object of the n.m.r. study was to determine whether water, in a two-component mixture with acetone, would ingress into a sample of VR at an increased rate. In this particular case spectroscopic results conclusively answer the question without recourse to imaging experiments. The experimental procedure was to immerse a cylinder of VR in a 1:1 by volume mixture of acetone and distilled water for two weeks. *Figure 11a* displays the spectrum obtained from the external undiffused solvent: approximately equal signal intensities are derived from the water (4.5 ppm) and acetone (1.5 ppm). *Figure 11b* shows the spectrum from the sample of VR; there is a peak corresponding to the acetone peak in *Figure 11a*, but none corresponding to the water peak. As a comparison, *Figure 11c* shows the spectrum from an identical sample of VR that had been immersed in acetone only; the acquisition parameters were as for *Figure 11b*, and the spectrum shows quite clearly that not only does water not diffuse at an enhanced rate into VR, but also that it effectively forms a preventive barrier to the diffusion of the acetone molecules.

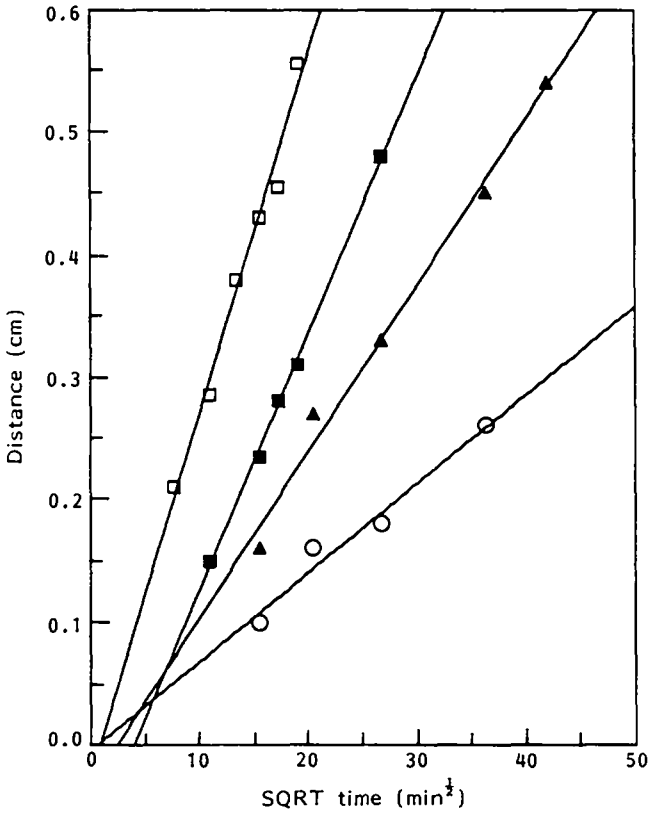

Figure 5 Comparison of the diffusion characteristics of four organic solvents through cylindrical samples of VR as measured from images corresponding to *Figure 4*: (□) benzene, (▲) isooctane, (■) cyclohexane, (○) acetone

The single-component diffusion coefficient of water through VR is several orders of magnitude less than that of acetone, and the physical mechanisms for this have been extensively studied[23,24]. The major cause for the extremely slow rate of diffusion of water through VR, compared to that which would be expected on molecular size considerations alone, is the occurrence of hydrophilic sites within the rubber, which act as a 'sink' for the water molecules and prevent further diffusion through the rubber matrix. One possible reason for the effective reduction in the rate of acetone diffusion is that the strong solvent–solvent interactions within these hydrophilic sinks also prevents the acetone from progressing further. In areas of the rubber where such sinks are not present, the acetone will diffuse normally but give rise to a

Table 2 N.m.r. properties of solvents ingressed in VR

Solvent	Chemical shift (ppm)	Scalar coupling (Hz)	T_1 (ms)	T_2 (ms)
Acetone	1.5	–	280	60
Benzene	7.2	–	2440	340
Cyclohexane	2.0	–	1290	300
Isooctane	1.3[a]	7.0[b]	1220[c]	95[c]

[a] Weighted average chemical shift
[b] Average scalar coupling constant
[c] Weighted average relaxation time

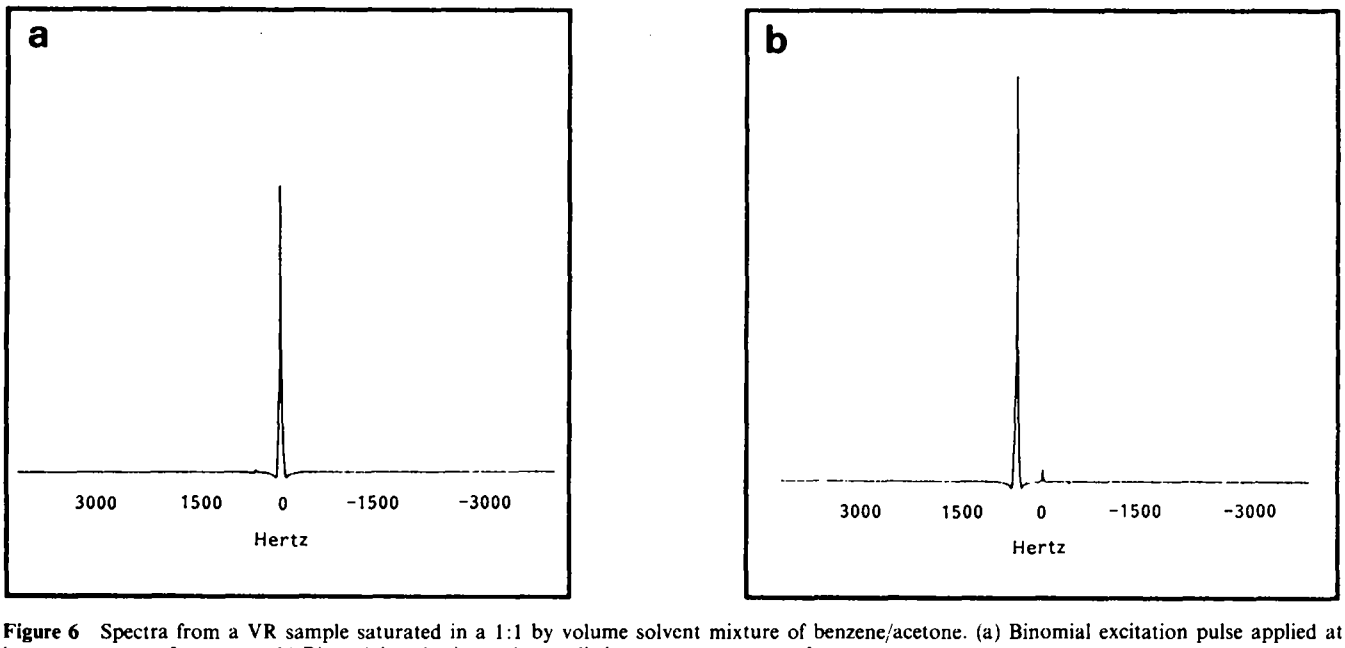

Figure 6 Spectra from a VR sample saturated in a 1:1 by volume solvent mixture of benzene/acetone. (a) Binomial excitation pulse applied at benzene resonant frequency. (b) Binomial excitation pulse applied at acetone resonant frequency

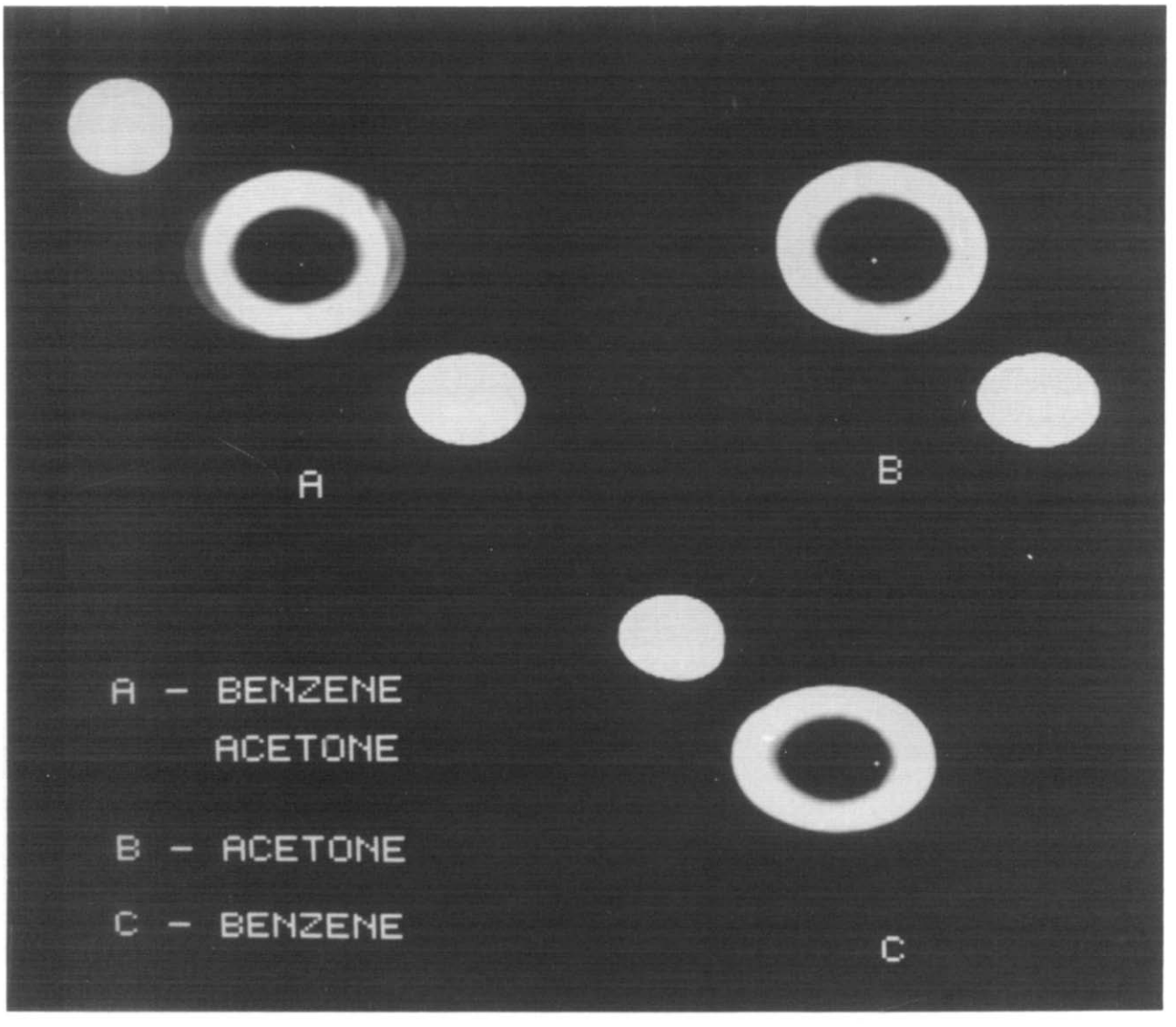

Figure 7 Images from a cylinder of VR, diameter 1.6 cm, after 4 h immersion in a 1:1 by volume benzene/acetone solvent mixture. Two external vials of pure solvent are also present. (A) Response from spin–echo sequence showing chemical shift artifact. (B) Response from acetone only, using binomial pulse centred at the benzene resonant frequency. (C) Response from benzene only. Imaging parameters: read-out gradient 4 kHz cm^{-1}, 128 incremental phase encode steps, slice thickness 0.4 cm, $T_E = 24.4$ ms, $T_R = 1$ s, one scan, total experimental time 2 min

considerably reduced signal intensity compared with single-component diffusion. It should be noted that this second example is likely to be a special case, involving as it does the unique mechanism of diffusion of water through rubbers, and that most organic solvent mixtures will give results similar in character to those determined for the benzene/acetone system.

A further area that has potential commercial implications is the diffusion of one solvent into a polymer that has previously been saturated with a second solvent. *Figure 12* shows a series of time course images from the diffusion of acetone into a cylinder of VR that had previously been saturated with benzene. Reference to the image taken after 360 min immersion in acetone shows that almost complete penetration had occurred This time is considerably shorter than that taken by either single-component benzene or single-component acetone ingress into a 'dry' VR sample. This increased rate of diffusion is due to the more open nature of the rubber matrix after swelling in benzene. This general result has important industrial repercussions in cases where a solvent deleterious to the physical properties of a particular polymer is miscible with a second, but benign, solvent.

SCALAR COUPLED EDITING

A second criterion for the editing of solvent responses is scalar coupling. If the chemical shifts of the two solvents overlap, due to either insufficient chemical shift dispersion, short values of T_2^*, or low B_0 homogeneity, neither selective excitation nor selective suppression techniques can be used. If, however, only one of the species contains resonances that are scalar coupled, then editing via the creation of multiple-quantum coherence (MQC) can be used.

The basic sequence to excite MQC is given below:

$$90_x\text{—}\tau\text{—}180\text{—}\tau \quad 90_x\text{—}t_1\text{—}90\text{—}\ \tau\ \text{—}180\text{—}\tau\text{—Acquire}$$

The effect of the first three radiofrequency pulses of this pulse sequence for a system of coupled spins is to generate MQC. This evolves during the t_1 period and is then

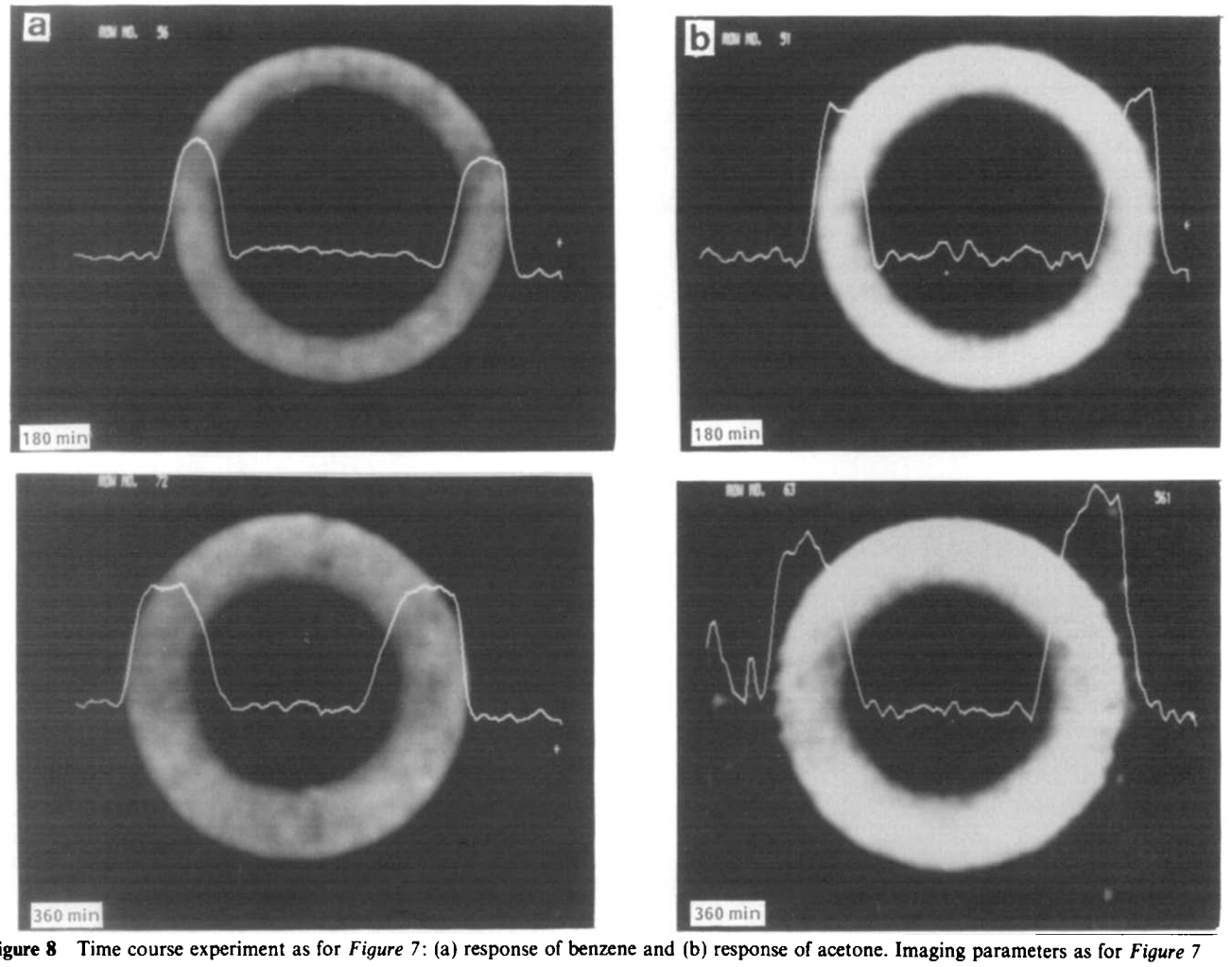

Figure 8 Time course experiment as for *Figure 7*: (a) response of benzene and (b) response of acetone. Imaging parameters as for *Figure 7*

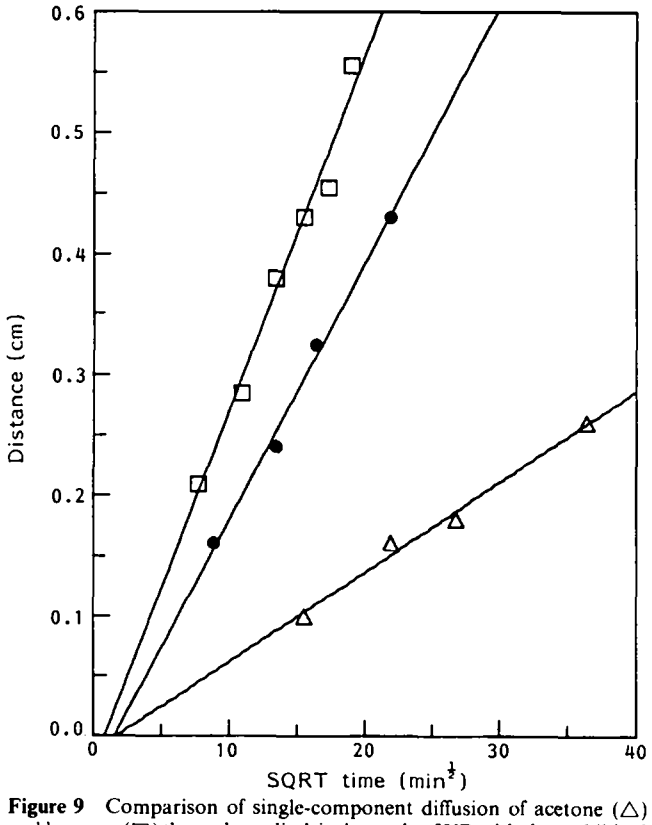

Figure 9 Comparison of single-component diffusion of acetone (△) and benzene (□) through a cylindrical sample of VR with that exhibited by a 1:1 by volume solvent mixture (●)

reconverted into single-quantum coherence (SQC) by the third 90° pulse; subsequent refocusing by the 180° pulse gives rise to a spin echo. However, for a non-coupled spin system the same sequence merely effects a series of spin rotations and also results in a spin echo. In order to create a scalar coupled filter, therefore, some means must be used to distinguish between SQC and MQC; the method used in the present study involves separation by magnetic field gradients.

A P-order MQC of spin k coupled to spin l will precess at a frequency ω_{MQC} given by:

$$\omega_{MQC} = P\omega_k \tag{7}$$

where ω_k is the SQC precession frequency of spin k, and is in turn given by:

$$\omega_k = \omega'_k + \gamma(1-\sigma_k)\,\Delta B_0(x, y, z) \tag{8}$$

where ω'_k is the Larmor frequency in the absence of any magnetic field inhomogeneities, $\Delta B_0(x, y, z)$ represents this spatial inhomogeneity and σ is the chemical shift of the nucleus. If a magnetic field G_z is now applied in the z direction, then the angular frequency of all nuclei with common coordinate z becomes:

$$\omega_z = \omega'_z + \gamma(1-\sigma_k)[\Delta B_0(x, y, z) + G_z \cdot z] \tag{9}$$

If the approximation $(1-\sigma)=1$ is applied, and it is assumed that all B_0 inhomogeneities are refocused during the sequence, then this equation can be reduced to:

$$\omega_z = \omega'_z + \gamma G_z \cdot z \tag{10}$$

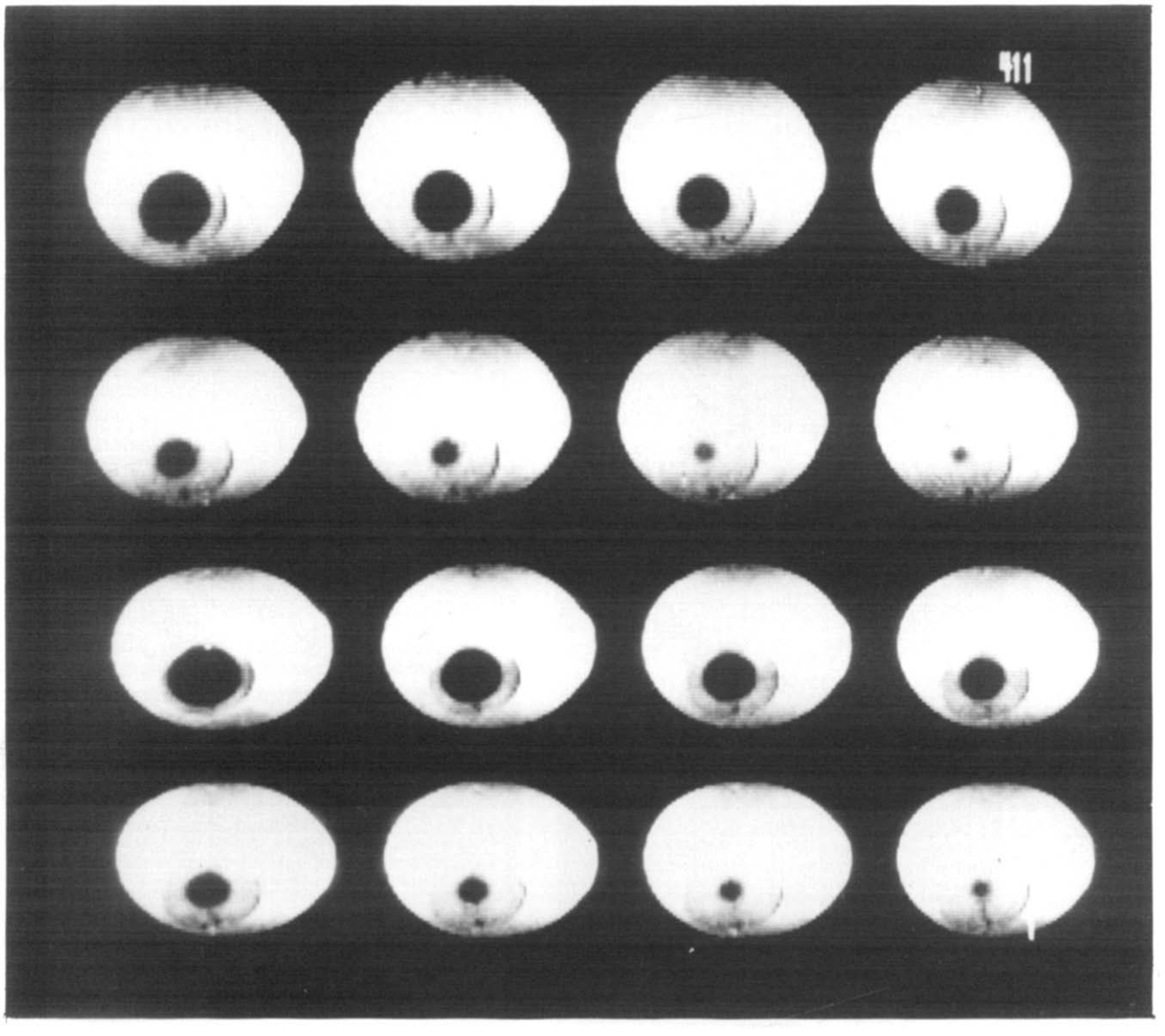

Figure 10 *In situ* diffusion of a benzene/acetone solvent mixture into a cylinder of VR, diameter 1.6 cm. The top eight chemical shift selective images correspond to the diffusion of benzene, and the lower eight to that of acetone. The time intervals after immersion are 90, 180, 270, 360, 450, 650, 800 and 890 min. Imaging parameters: read-out gradient 1 kHz cm^{-1}, 128 incremental phase encode steps, slice thickness 0.4 cm, $T_E = 28.8$ ms, $T_R = 1$ s, one scan, total experimental time 2 min

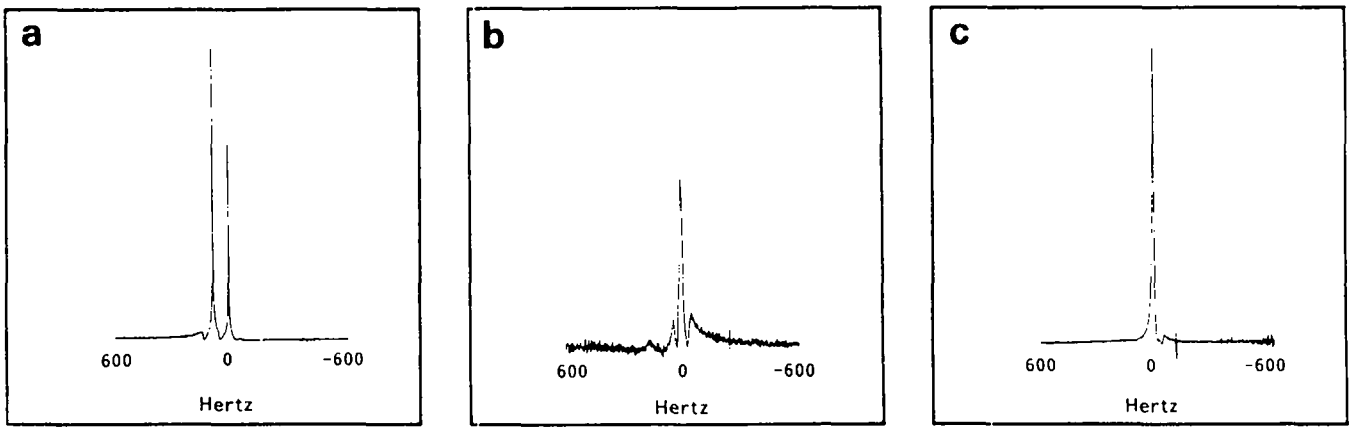

Figure 11 Spectra taken after two weeks immersion of a sample of VR in a 1:1 by volume mixture of acetone and water. (a) Spectrum from external liquid. (b) Spectrum from the sample of VR showing only a peak corresponding to the acetone resonance. (c) Reference spectrum from an identical sample of VR after immersion in acetone only. One scan was acquired in each case

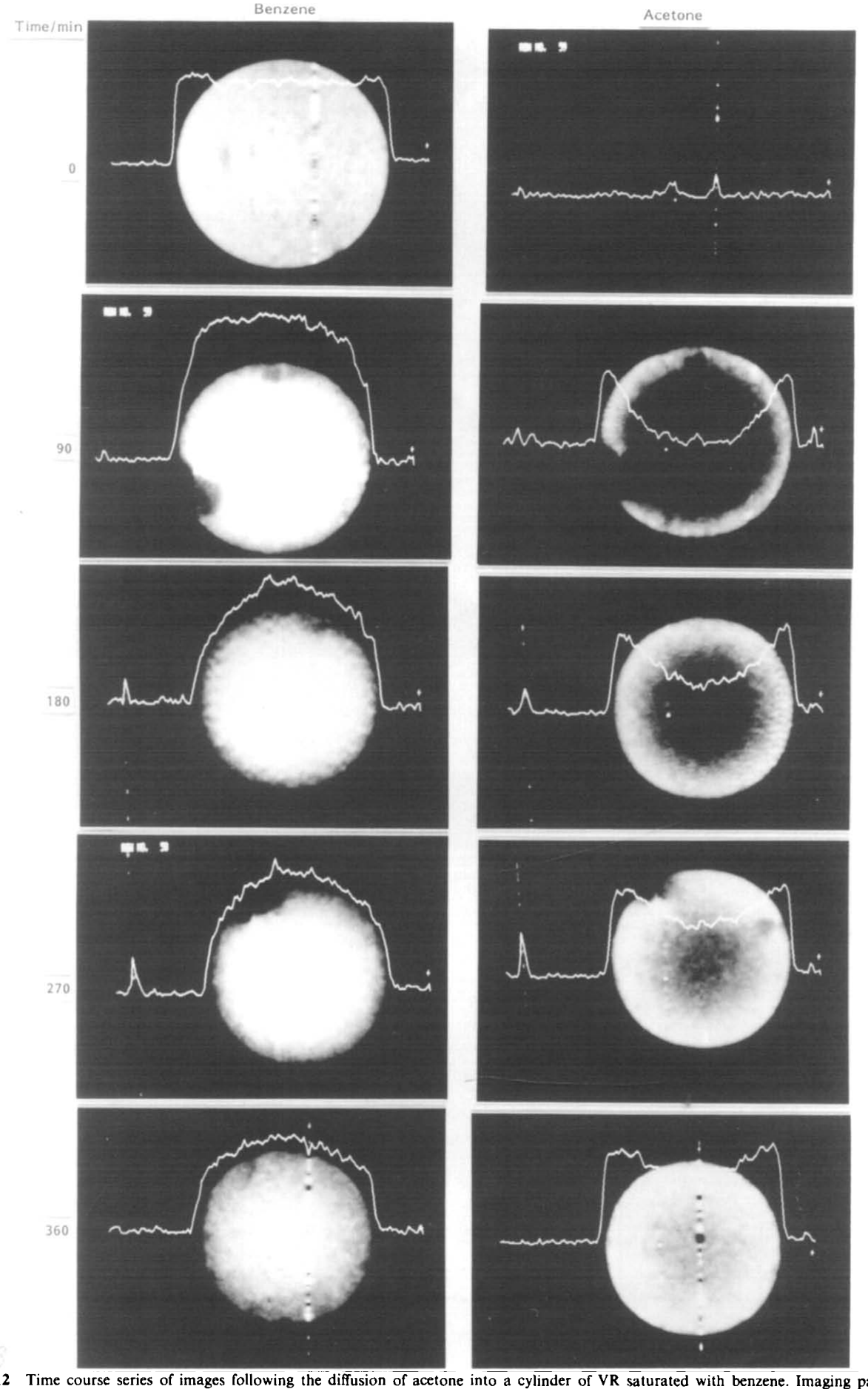

Figure 12 Time course series of images following the diffusion of acetone into a cylinder of VR saturated with benzene. Imaging parameters: read-out gradient 2.5 kHz cm^{-1}, 128 incremental phase encode steps, slice thickness 0.4 cm, $T_E = 28.8$ ms, $T_R = 1$ s, one scan, total experimental time 2 min

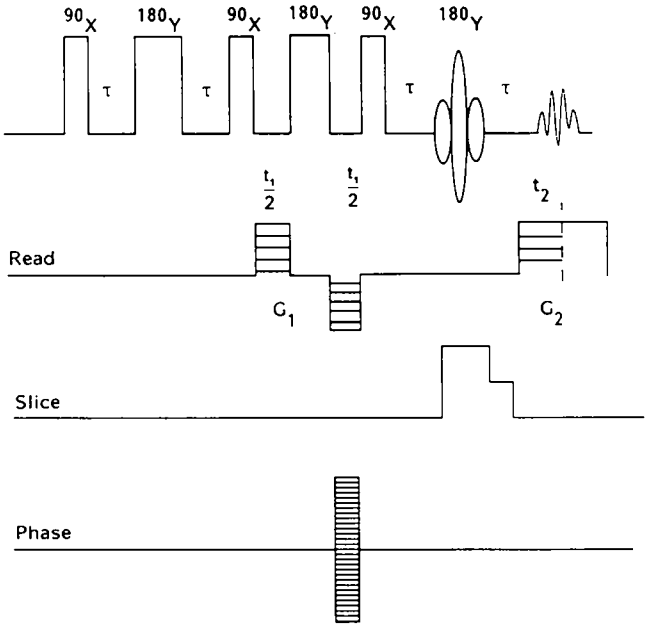

Figure 13 Imaging sequence for selective detection of multiple-quantum coherence

Substitution into equation (7) leads to:

$$\omega_{MQC} = P(\omega_z' + \gamma G_z \cdot z) \quad (11)$$

If only the gradient term is considered then the dephasing caused by a given gradient strength is directly proportional to the order of MQC. This property can be used to separate different orders of MQC, and in particular to suppress SQC.

The imaging sequence used is shown in *Figure 13*, an adaptation of that of Szeverenyi and Haake[25]. A 180° pulse is inserted at time $t_1/2$ after the start of MQC evolution in order to refocus both chemical shift and B_0 inhomogeneity. In the case of double-quantum coherence (DQC) the total gradient encoding from the dephasing read gradient is $2G_1t_1$. The rephasing gradient G_2 is set such that, at the middle of the acquisition window, $2G_1t_1 = G_2t_2$, and the gradient strengths are arranged such that the DQC gradient-induced echo coincides with multiplet refocusing at a time $(4\tau + t_1)$ after the initial 90° pulse. Any SQC echo that forms will only experience gradient encoding from the dephasing read gradient of G_1t_1, and will thus be refocused by the G_2 gradient at a time earlier than the DQC echo and can be suppressed by ensuring that this echo does not occur within the acquisition window.

This sequence can be used to separate the responses of isooctane, which possesses scalar coupled proton nuclei and can hence give rise to MQC, from those of cyclohexane, which cannot. The resonances of these two solvents overlap in the chemical shift domain and thus cannot be separated by selective excitation or suppression techniques. *Figure 14* shows a time course series of images based on both single-quantum coherence and double-quantum coherence obtained from the immersion into isooctane of a cylinder of VR that had previously been saturated in cyclohexane. It is far from easy to determine the exact spatial location of the isooctane solvent front in those images arising from the single-quantum coherence; however, the fronts are much more sharply defined in those arising from the double-quantum coherence. Once again the diffusion rate of the ingressing solvent is far greater in the two-component mixture than either of the diffusion rates of the single-component systems.

EDITING VIA RELAXATION TIMES

If two species exhibit identical scalar coupling behaviour, and in addition cannot be separated on the basis of chemical shift, then a third potential approach to editing is to utilize differences in relaxation times, shown in *Table 2*. If an inversion–recovery module (180°–τ) precedes the 90° excitation pulse of the spin–echo imaging experiment, then the signal intensities of species A and B are given respectively by:

$$S_A = S_0\left[\exp\left(-\frac{T_E}{T_{2A}}\right)\right]\left[1 - 2\exp\left(-\frac{\tau}{T_{1A}}\right)\right]$$

$$S_B = S_0\left[\exp\left(-\frac{T_E}{T_{2B}}\right)\right]\left[1 - 2\exp\left(-\frac{\tau}{T_{1B}}\right)\right]$$

assuming full relaxation between successive inversion pulses. If the value of τ is set to $T_{1A}/\ln 2$ then the signal intensity from species A will be nulled whereas, providing that $T_{1A} \neq T_{1B}$, there will be residual intensity arising from the B spins, and vice versa. This then would appear to be a convenient way of editing the nuclear responses; unfortunately, the problem with this approach is that the relaxation behaviour of the individual liquids in a two-component system is considerably altered with respect to the single-component system; *Table 3* shows two examples of this. The results show that, in samples containing regions where only one solvent is present, and also areas where both solvents are present, there will be a spread of different relaxation times dependent on the relative concentrations of the two components. This precludes accurate nulling of either of the responses across the entire sample. A similar analysis applies when the feasibility of suppressing signals from components with short T_2 values is considered. One possible method is simply to use an extended value of T_E within the spin–echo sequence. The single-component T_2 values shown in *Table 2* suggest that this would be a suitable method of suppressing the acetone resonances, for example, in a mixed solvent system of acetone and cyclohexane. However, as shown in *Table 4*, the T_2 values of a two-component system change from those of a single-component system in a similar fashion to the T_1 values, and will be concentration-dependent as before.

The conclusions drawn from these relaxation data must be that differential relaxation times are not an effective criterion for editing of the individual responses, and that some other method must be found if the responses from, for example, cyclohexane and acetone are to be separated. Such a method is discussed in the following section.

ISOTOPIC SUBSTITUTION

The problems associated with differentiating species exhibiting identical scalar coupling properties, and whose resonances in the frequency domain cannot be resolved by chemical shift imaging methods, can potentially be solved by the application of isotopic substitution.

The low sensitivity of the deuterium nucleus, 9×10^{-7} with respect to protons, dictates that the direct detection

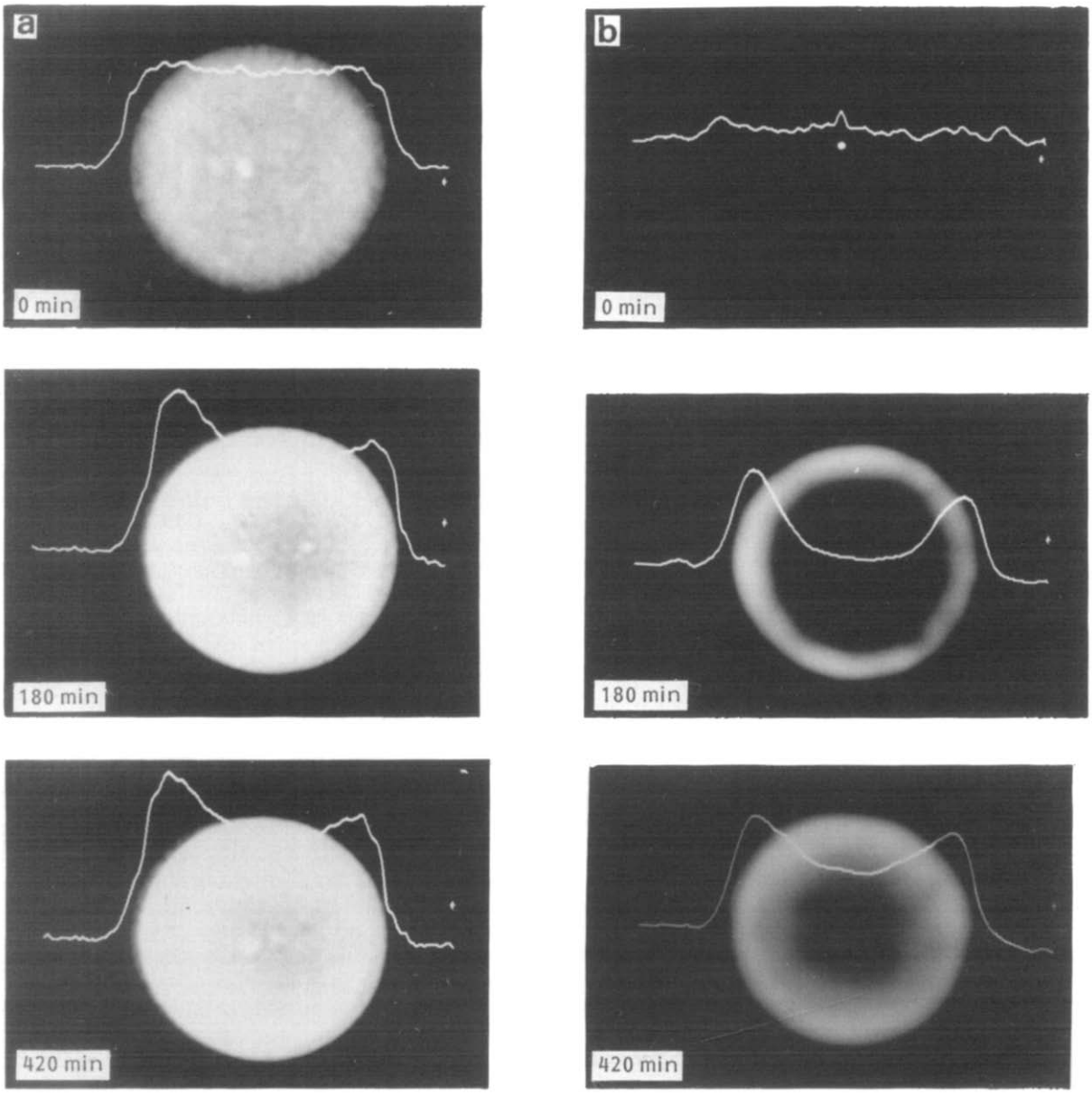

Figure 14 Time course experiment following the ingress of isooctane into a sample of VR previously saturated with cyclohexane. (a) Single-quantum response from nuclei in both solvents. (b) Double-quantum response from scalar coupled nuclei in the isooctane only. Imaging parameters: read-out gradient 2.5 kHz cm^{-1}, 128 incremental phase encode steps, slice thickness 0.8 cm, $T_E = 28.8$ ms, $T_R = 1$ s. One scan was acquired for the SQC image and four scans for the DQC image

Table 3 Solvent spin–lattice relaxation times

	Single-component	Two-component (1:1)
Cyclohexane	1.29 s	1.85 s
Acetone	0.28 s	1.19 s
Benzene	2.44 s	2.65 s
Acetone	0.28 s	1.26 s

Table 4 Solvent spin–spin relaxation times

	Single-component	Two-component (1:1)
Cyclohexane	300 ms	480 ms
Acetone	60 ms	230 ms
Benzene	340 ms	380 ms
Acetone	60 ms	210 ms

of this particular nucleus is not practicable on a timescale compatible with the diffusion processes studied in this work, and therefore this means of isotopic substitution can only be used in a 'negative' sense. For example, a mixture of cyclohexane and acetone-d_6, in which all of the protons of acetone have been replaced by deuterium nuclei, will only give rise to a proton signal from the cyclohexane molecules. An important point to note is that the intermolecular solvent–solvent and solvent–polymer interactions are very similar for acetone-d_6 and acetone; this similarity in physicochemical properties is borne out by the respective boiling points of 55.5 and 56.5°C, indicating that the intermolecular van der Waals forces as well as the physical sizes of the two molecules are very similar. This supports the assumption that the diffusion kinetics displayed by the two solvents will be virtually identical.

Figure 15 shows a time course series of images, which

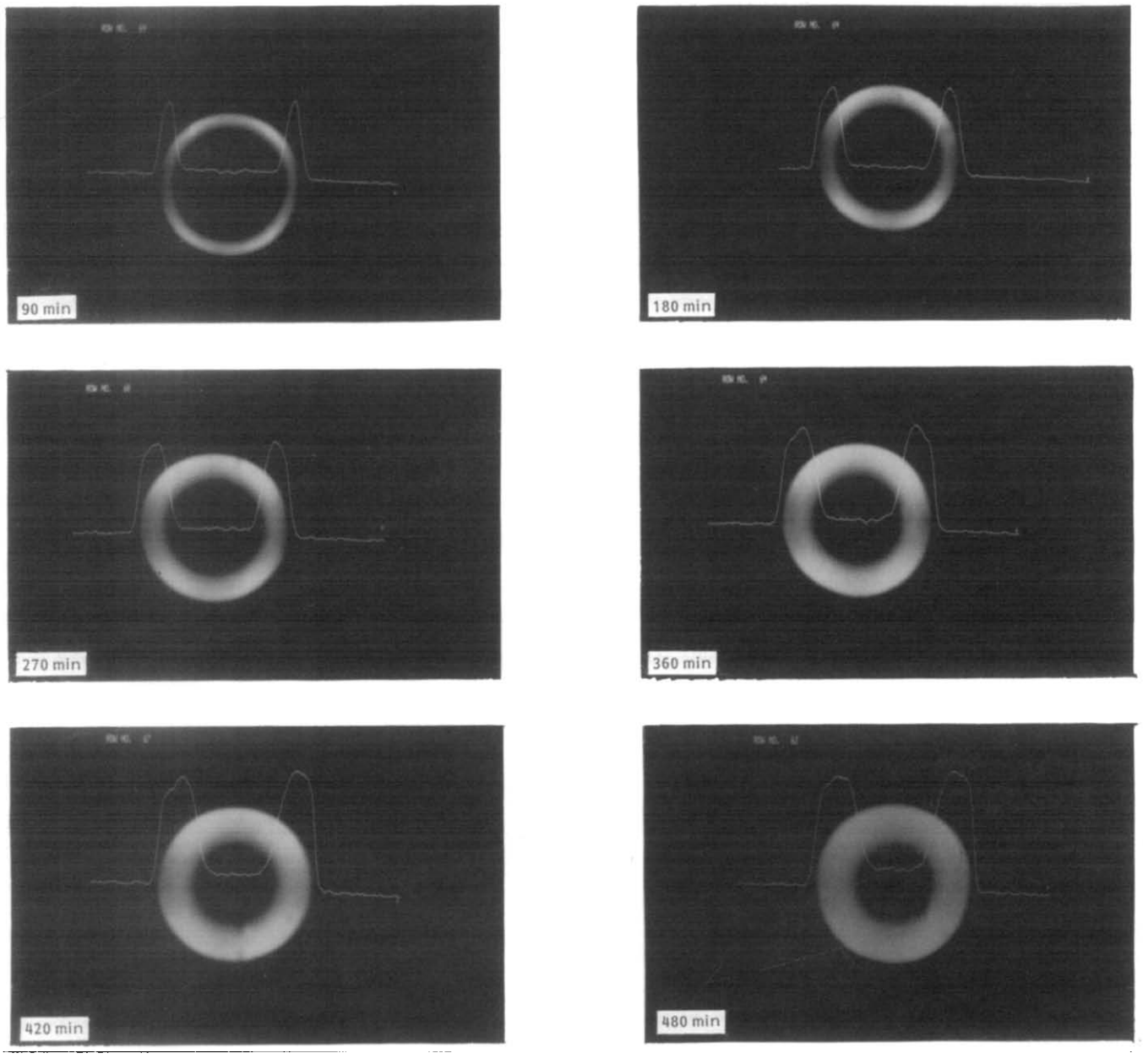

Figure 15 Time course proton images of cyclohexane diffusing into a cylinder of VR, diameter 2 cm, previously saturated with acetone-d_6. Imaging parameters: read-out gradient 2.5 kHz cm^{-1}, 128 incremental phase encode steps, slice thickness 0.4 cm, $T_E = 28.8$ ms, $T_R = 1$ s, two scans, total experimental time 4 min

follow the ingress of cyclohexane into a cylinder of VR, dimensions $2 \times 2 \times 2.5$ cm, that had previously been saturated in acetone-d_6. In this case the concentration profiles are far steeper than those derived either for the diffusion of acetone into a benzene-saturated cylinder of VR, or isooctane into a cyclohexane-saturated cylinder. A second point of note is that the penetration rate of the cyclohexane is approximately 2.5 times that of the single-component solvent into a dry sample of VR, which is a far smaller increase than recorded in the two previous experiments where the sample had been presaturated. The reason for both of these observations is that acetone is a very poor swelling solvent, and therefore the VR matrix is relatively little changed in physical terms by the ingress of acetone. In contrast, when the rubber has been previously ingressed with a swelling solvent such as benzene or cyclohexane, the rubber lattice is considerably stretched, leading to a much more open and porous molecular structure and hence to a faster rate of diffusion for the ingressing solvent.

A potential alternative to deuterium labelling is that of substitution, either full or partial, of protons in a molecule by fluorine nuclei. The sensitivity and natural abundance of fluorine are very similar to protons, and direct detection of the fluorinated species is therefore viable. Problems, however, can arise from the considerable change in physical properties that substitution of fluorine nuclei for protons can induce. For example, perfluoroacetone is a gas and perfluorocyclohexane is a solid! Such changes in physical properties afforded by such substitution means that great care must be taken to ensure that the diffusion kinetics of the fluorinated

and protonated solvents are the same in order to carry out such experiments; in general, this will not be a viable approach.

SUMMARY

Four techniques have been evaluated for the study of two-component diffusion through samples of VR. Chemical shift selective methods were used for an acetone/benzene mixture, and both *in situ* and *ex situ* experiments showed that each component ingressed at the same rate despite their very different single-component penetration rates. In contrast, diffusion of an acetone/water mixture did not enhance the rate of water penetration, and indeed considerably reduced that of acetone; the reasons for this related to the particular mechanism of water diffusion through rubber samples. Diffusion of acetone into a sample of VR presaturated with benzene proceeded at a rate greater than that of either single component owing to the more open nature of the rubber matrix after swelling in benzene.

Scalar coupled editing, via the creation of multiple-quantum coherence, was used to follow the diffusion of isooctane through a sample of VR presaturated in cyclohexane. Once again the rate of diffusion was much greater than that of the single components, and can similarly be attributed to the change in the physical nature of the rubber on swelling.

Editing via relaxation times was shown to be impractical because of the strong dependence of the relaxation times on the relative concentrations of the two components. Therefore, isotopic substitution of deuterium nuclei for protons was used to separate the responses from acetone and cyclohexane, which could not be edited by any of the previous methods.

All experiments were carried out at 2.0 T in a 31 cm bore Oxford Instruments horizontal cryomagnet controlled by a Biospec I console (Oxford Research Systems, Bruker).

ACKNOWLEDGEMENTS

It is a pleasure to thank Dr Herchel Smith for an endowment (LDH) and a research studentship (AGW). We are also indebted to Dr Adrian Carpenter and Ping Gao for technical advice and discussion. We would also like to thank Professor Soon Ng and the Malaysian Rubber Company for providing samples of vulcanized rubber.

REFERENCES

1 Alfrey, A., Gurnee, E. F. and Lloyd, W. G. *J. Polym. Sci. (C)* 1966, **12**, 249
2 MacBain, J. W. and Bakr, A. M. *J. Am. Chem. Soc.* 1926, **48**, 690
3 King, G. *Trans. Faraday Soc.* 1945, **41**, 325
4 Prager, S. and Long, F. A. *J. Am. Chem. Soc.* 1951, **73**, 4072
5 Garrett, T. A. and Park, G. S. *J. Polym. Sci. (C)* 1966, **16**(1), 601
6 Barrer, R. M., Barrie, J. A. and Slater, J. *J. Polym. Sci.* 1958, **27**, 177
7 Rosen, B. *J. Polym. Sci.* 1959, **35**, 335
8 Robinson, C. *Proc. R. Soc. (A)* 1950, **204**, 339
9 Crank, J. and Robinson, C. *Proc. R. Soc. (A)* 1950, **204**, 549
10 Hutcheon, A. T., Kokes, R. J., Hoard, J. L. and Long, F. A. *J. Chem. Phys.* 1952, **20**, 1232
11 Taylor, R. L., Hermann, D. B. and Kemp, A. R. *Ind. Eng. Chem.* 1936, **28**, 1255
12 Long, F. A. and Richman, D. *J. Am. Chem. Soc.* 1960, **82**, 509
13 Bueche, F., Cashin, W. M. and Debye, P. V. *J. Chem. Phys.* 1952, **20**, 1956
14 Gummerson, R. J., Hall, C., Hoff, W. D., Hawkes, R., Holland, G. N. and Moore, W. S. *Nature* 1979, **281**, 56
15 Rothwell, W. P., Holecek, D. R. and Kershow, J. A. *J. Polym. Sci., Polym. Lett. Edn.* 1984, **22**, 241
16 Weisenberger, L. A. and Koenig, J. L. *ACS Polym. Prepr.* 1988, **29**, 98
17 Chu, S. and Foxall, D., 'Twenty Ninth Experimental NMR Conference', 1988, p. 132
18 Blackband, S. and Mansfield, P. *J. Phys. (C)* 1986, **19**, L49
19 Webb, A. G. and Hall, L. D. *Polym. Rep.* 1990, **30**, 425
20 Gao, P., Ph.D. thesis, Cambridge University, 1990
21 Webb, A. G. and Hall, L. D. *Polym. Rep.* 1990, **30**, 422
22 Hore, P. J. *J. Magn. Reson.* 1983, **55**, 283
23 Shatzberg, P. *J. Phys. Chem.* 1963, **67**, 776
24 Fedors, R. F. *Polymer* 1980, **21**, 207
25 Szeverenyi, N. M. and Haake, E. M. *J. Comput. Assist. Tomogr.* 1986, **8**, 484